Monthly Notices
of the
ROYAL ASTRONOMICAL SOCIETY

MNRAS **487,** L47–L52 (2019)
Advance Access publication 2019 May 14

doi:10.1093/mnrasl/slz070

The Fall of a Giant. Chemical evolution of Enceladus, alias the Gaia Sausage

Fiorenzo Vincenzo,[1]★ Emanuele Spitoni,[2] Francesco Calura,[3] Francesca Matteucci,[4,5,6] Victor Silva Aguirre,[2] Andrea Miglio[1] and Gabriele Cescutti[5]

[1]*School of Physics and Astronomy, University of Birmingham, Edgbaston B15 2TT, UK*
[2]*Stellar Astrophysics Centre, Department of Physics and Astronomy, Aarhus University, Ny Munkegade 120, DK-8000 Aarhus C, Denmark*
[3]*INAF, Osservatorio Astronomico di Bologna, Via Gobetti 93/3, I-40129 Bologna, Italy*
[4]*Dipartimento di Fisica, Sezione di Astronomia, Universita' di Trieste, via G.B. Tiepolo 11, I-34131 Trieste, Italy*
[5]*INAF, Osservatorio Astronomico di Trieste, via G.B. Tiepolo 11, I-34131 Trieste, Italy*
[6]*INFN, Sezione di Trieste, Via Valerio 2, I-34100 Trieste, Italy*

Accepted 2019 May 7. Received 2019 May 1; in original form 2019 March 8

ABSTRACT

We present the first chemical evolution model for Enceladus, alias the Gaia Sausage, to investigate the star formation history of one of the most massive satellites accreted by the Milky Way during a major merger event. Our best chemical evolution model for Enceladus nicely fits the observed stellar [α/Fe]–[Fe/H] chemical abundance trends, and reproduces the observed stellar metallicity distribution function, by assuming low star formation efficiency, fast infall time-scale, and mild outflow intensity. We predict a median age for Enceladus stars $12.33^{+0.92}_{-1.36}$ Gyr, and – at the time of the merger with our Galaxy ($\approx$10 Gyr ago from Helmi et al.) – we predict for Enceladus a total stellar mass $M_\star \approx 5 \times 10^9\,M_\odot$. By looking at the predictions of our best model, we discuss that merger events between the Galaxy and systems like Enceladus may have inhibited the gas accretion on to the Galaxy disc at high redshifts, heating up the gas in the halo. This scenario could explain the extended period of quenching in the star formation activity of our Galaxy about 10 Gyr ago, which is predicted by Milky Way chemical evolution models, in order to reproduce the observed bimodality in [α/Fe]–[Fe/H] between thick- and thin-disc stars.

Key words: stars: abundances – Galaxy: abundances – Galaxy: evolution – Galaxy: formation – galaxies: individual: Enceladus – galaxies: individual: Gaia Sausage.

1 INTRODUCTION

Understanding the past mass assembly history and the dynamical evolution of the stellar components of our Galaxy by looking at its stellar halo is one of the major challenges of contemporary astrophysics (e.g. Morrison et al. 2000; Prantzos 2008; Deason et al. 2017; Di Matteo et al. 2018; Hayes et al. 2018; Helmi et al. 2018). During its evolution across cosmic times, it is highly likely that the Milky Way (MW) was surrounded by many galaxy companions, which suffered from strong tidal interactions, being continuously stripped of their stars and gas by the gravitational pulling forces; a large fraction of these companions are today seen as stellar streams, or dispersed tidal debris in the velocity- and chemical-abundance spaces (Helmi et al. 1999, 2018; Kruijssen et al. 2019; Gallart et al. 2019; Simion, Belokurov & Koposov 2019).

From a theoretical point of view, the standard Λ-cold dark matter (CDM) paradigm for the formation and evolution of the structures in the cosmos predicts a large number of satellite galaxies around massive disc galaxies like the Milky Way. In particular, the MW dark matter (DM) halo should have formed from the accretion of filamentary structures and from the coalescence of many small DM haloes at high redshifts, with the mass of the accreted systems increasing – on average – as a function of time (Helmi & White 1999; Bullock, Kravtsov & Weinberg 2001).

The absence of a large number of dwarf galaxies gravitationally bound to the MW was one of the major discrepancies between observations and model predictions (Klypin et al. 1999), until the advent of the Sloan Digital Sky Survey (SDSS) and the Dark Energy Survey (DES), which – in the last 15 yr – discovered an impressive

★ E-mail: f.vincenzo@bham.ac.uk

amount of new dSphs and ultra-faint dwarfs (UfDs) around the Milky Way (Simon 2019).

Thanks to the SDSS and – more recently – to the DES and SDSS-Gaia, many stellar streams were discovered in the inner MW halo as faint substructures (Belokurov et al. 2006; Myeong et al. 2018a; Shipp et al. 2018). The most studied of these stellar streams is associated with Sagittarius dSph, and was intensively investigated in terms of its chemical abundances, kinematics, and stellar population properties by many independent studies over the years (Ibata et al. 2001; Majewski et al. 2003; Newberg et al. 2003; de Boer, Belokurov & Koposov 2015). Other stellar streams were later the subject of similar intense investigations (Koposov, Belokurov & Torrealba 2017; de Boer, Belokurov & Koposov 2018a; de Boer et al. 2018b; Koposov et al. 2019).

Recent unprecedented analysis of the seven-dimensional Gaia-SDSS catalogue revealed a metal-rich component in the inner Galaxy halo, which shows a peculiar elongated shape along the horizontal axis of the velocity ellipsoid, as given by the azimuthal stellar velocity component, v_θ, versus the radial velocity component, v_r (Belokurov et al. 2018). This renamed 'sausage' in the velocity-space is probably due to relatively metal-rich stars compared to the Galaxy halo (with metallicities $Z \approx Z_\odot/10$), which have also large velocity anisotropy ($\beta \approx 0.95$) (see Myeong et al. 2018b; Fattahi et al. 2019). This 'sausage' represents the dynamical record in the velocity-space of a head-on major collision that the MW experienced more than 10 Gyr ago with a quite massive dwarf galaxy. We also address the readers to the works of Iorio & Belokurov (2019), for a detailed study of the dynamical structure of the MW halo by making use of RR Lyrae, and Di Matteo et al. (2018), Haywood et al. (2018), and Mackereth et al. (2019a), for interesting studies on the connection between the Gaia Sausage and the MW accretion history from chemical and kinematical points of view, using different techniques. The progenitor (now disrupted) galaxy of this 'sausage' in the velocity-space is now called Gaia Enceladus, or Gaia Sausage.

A sample of confirmed Gaia Sausage member stars is present in the catalogue of the APO Galactic Evolution Experiment (APOGEE). These stars were selected by Helmi et al. (2018), to show that – in the [α/Fe]–[Fe/H] chemical abundance diagram – they have properties very similar to those of some dSph stars, i.e. typically lower [α/Fe] values than metal-poor MW halo stars (see, also, Hayes et al. 2018 for a detailed study).

Interestingly, Nissen & Schuster (2010) showed that, with VLT/UVES and NOT/FIES observations, the metal-rich tail of the Galactic halo is characterized by two distinct populations of stars. The authors explained such a dichotomy by proposing that the low-[α/Fe] stellar component was probably accreted from dwarf galaxies. Finally, before the release of Gaia DR2, Fernández-Alvar et al. (2018) investigated the average star formation rate (SFR) and initial mass function (IMF) in a very similar sample of APOGEE stars with respect to that later selected by Helmi et al. (2018) for Enceladus, finding two distinct [α/Fe]-sequences.

In this Letter, we present the first attempt of modelling in detail the chemical evolution of Enceladus, fitting our chemical evolution model to reproduce the observed [α/Fe]–[Fe/H] and the metallicity distribution function (MDF) of the stars in Enceladus. This Letter is structured as follows. In Section 2 we describe the adopted chemical evolution model and the main features of the best model for Enceladus. In Section 3 we present the results of our study. Finally, in Section 4, we draw our conclusions.

2 THE CHEMICAL EVOLUTION MODEL

We develop a chemical evolution model to reproduce the abundances in Enceladus, by assuming the same set of stellar nucleosynthetic yields as in François et al. (2004) for massive stars (dying as core-collapse SNe), Type Ia SNe, and asymptotic giant branch stars. For Type Ia SNe, we assume the single degenerate scenario, with the same prescriptions as in Matteucci & Recchi (2001). In our model, we solve a set of differential equations, and assume stellar nucleosynthetic yields, which are the same as those of the MW two-infall chemical evolution model of Spitoni et al. (2019). The stellar yields and Type Ia SN model are usually selected with the aim of reproducing the observed MW chemical abundances, and later applied to study also external galaxies. We follow this approach, relying on the nucleosynthesis assumptions of Spitoni et al. (2019).

We assume that Enceladus forms at high redshift from the rapid collapse of primordial gas in the intergalactic medium (IGM). The infall rate of gas from the IGM into the Enceladus potential well is of the form $\mathcal{I}(t) = A\, e^{-t/\tau_{\rm inf}}$, where $\tau_{\rm inf}$ is the infall time-scale, a free parameter of the model, and the normalization constant, A, fixes the total amount of gas mass accreted from the IGM during the galaxy lifetime, which is the so-called infall mass, $M_{\rm inf}$. The SFR in our model follows a linear Schmidt–Kennicutt law, i.e. SFR = SFE $\times$ $M_{\rm gas}$, with SFE being the star formation efficiency. We also assume galactic winds to develop when the thermal energy of the gas – heated by stellar winds and SNe – exceeds the binding energy of the gas due to the galaxy potential well, as in Bradamante, Matteucci & D'Ercole (1998). The intensity of the outflow rate is directly proportional to the SFR, namely $\mathcal{O}(t) = w \times {\rm SFR}(t)$, where w is the mass loading factor, a free parameter of the model. In order to compute the binding energy, we assume that the mass of the DM halo is $M_{\rm DM} = 10 \times M_{\rm inf}$. Finally, in our model we assume the stellar lifetimes of Padovani & Matteucci (1993) and the initial mass function (IMF) of Kroupa, Tout & Gilmore (1993), defined in the mass range between 0.1 and 100 $M_\odot$.

We create a grid of $\sim$17 500 models by varying the main free parameters (SFE, w, and $\tau_{\rm infall}$), in order to reproduce the trend of the observed [α/Fe]–[Fe/H] (Helmi et al. 2018). In our best model, we assume SFE = 0.42 Gyr^{-1}, $\tau_{\rm inf} = 0.24$ Gyr, and the infall law is normalized to have a total amount of accreted gas mass $M_{\rm infall} = 10^{10}$ $M_\odot$. The mass loading factor does not play an important role in our models for Enceladus, because the wind is predicted to occur relatively late in the galaxy evolution, at [Fe/H] abundances larger than those observed for Enceladus stars by Helmi et al. (2018), we assume in our fiducial model $w = 0.5$, but in Section 3 we will show our results for $w = 0$, 0.5, and 1.0.

2.1 Exploring the parameter space

On the one hand, our predictions for [α/Fe]–[Fe/H] and the MDF are highly sensitive to the SFE, which determines the time (and [Fe/H] value) when the first Type Ia SNe explode, causing [α/Fe] to sharply decrease as a function of [Fe/H]. On the other hand, the infall time scale cannot be precisely constrained if we only look at [α/Fe]–[Fe/H]. Nevertheless, the MDF – which is an important observational constraint to reproduce – strongly depends on the assumed infall time scale; this is shown in Fig. 1, where our estimator to evaluate the goodness of the models to reproduce [α/Fe]–[Fe/H] is drawn as a function of SFE and $\tau_{\rm inf}$. The best model, reproducing both the observed [α/Fe]–[Fe/H] and the

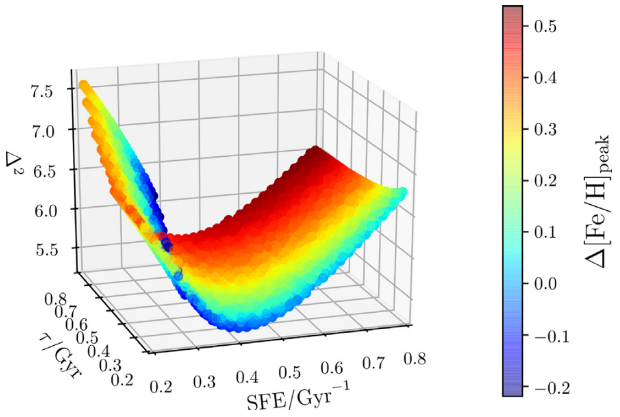

Figure 1. The adopted figure-of-merit to evaluate the goodness of our models in reproducing the observed [α/Fe]–[Fe/H] of Enceladus stars ($\Delta^2 \propto \sum_i \left[[\alpha/\mathrm{Fe}]([\mathrm{Fe/H}]_i)^2_{\rm mod} - [\alpha/\mathrm{Fe}]([\mathrm{Fe/H}]_i)^2_{\rm obs}\right]/\sigma_i^2$) as a function of SFE and $\tau_{\rm inf}$. The colour coding represents the difference between the [Fe/H] of the MDF peak of each model and that of the best model, which reproduces both the observed stellar [α/Fe]–[Fe/H] and the observed MDF (the absolute minimum at SFE = 0.42 Gyr^{-1} and $\tau_{\rm inf}$ = 0.24 Gyr).

observed MDF, corresponds to the minimum at SFE= 0.42 Gyr^{-1} and $\tau_{\rm inf}$ = 0.24 Gyr.

3 RESULTS

In Fig. 2(a) we compare our fiducial chemical evolution model for Gaia Enceladus with the observed data of Helmi et al. (2018). The colour coding in the figure corresponds to the predicted SFR along the chemical evolution track as the system evolves as a function of time. Given the relatively low SFE of the best model, we can reproduce the overall declining trend of Enceladus stars in the [α/Fe]–[Fe/H] abundance diagram, which is due to large contribution of Fe from Type Ia SNe, contributing already at such low [Fe/H]. Our model can reproduce the observed trend in the Helmi et al. (2018) data set. Our model indicates that, when most of the observed stars formed, Enceladus was characterized by SFR values between ∼1 and 3.5 M$_\odot$ yr^{-1}.

In Fig. 2(b) we compare the MDF of our fiducial chemical evolution model for Enceladus with the data set of Helmi et al. (2018). To show that the mass loading factor plays a marginal role for the bulk of the chemical evolution of Enceladus, we show models with different values of w, from $w = 0$ (no wind) to $w = 1.0$. We find that the median iron abundance of our fiducial model with $w = 0.5$ is [Fe/H] = $-1.26^{+0.82}_{-1.06}$ dex, in very good agreement with the observed median value [Fe/H]$_{\rm obs}$ = $-1.21^{+0.59}_{-0.49}$ dex. The predicted MDFs show a large spread in the iron abundances, while the data of Helmi et al. (2018) do not cover the very low metallicity regime. However, it is worth to stress that it is very difficult to obtain very accurate spectroscopic chemical abundance measurements for very metal-poor stars (see the discussion in Placco et al. 2018). Secondly, it is plausible that a non-negligible fraction of the oldest, most metal poor stars formed in Enceladus did not reach the inner Galactic halo; the oldest stellar components of galaxies typically have, in fact, the highest velocity dispersion (Sanders & Das 2018; Ting & Rix 2018; Mackereth et al. 2019b).

From the analysis of the best model, we can reconstruct the total stellar and gas mass of Enceladus before the collision with the MW (which happened ∼10 Gyr ago, according to Helmi et al. 2018), as well as the ages of Enceladus stars. In Fig. 2(c), we show our

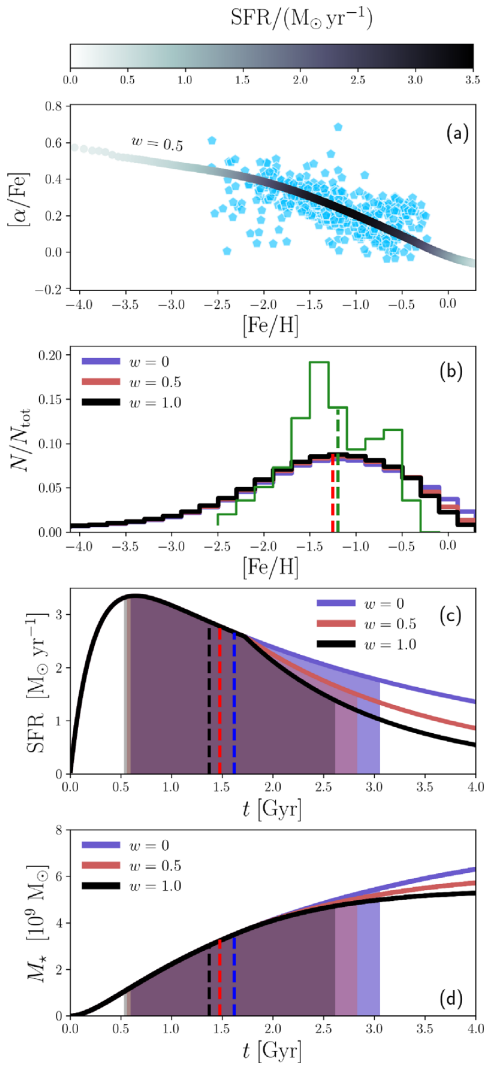

Figure 2. (a) Observed [α/Fe]–[Fe/H] for Enceladus from Helmi et al. (2018) (light blue pentagons), compared with our fiducial chemical evolution model with $w = 0.5$. The colour code indicates the intensity of the SFR. (b) The MDF of our fiducial model for Enceladus, by varying the mass loading factor, w. The green histogram corresponds to the data of Helmi et al. (2018). The vertical dashed lines indicate the median [Fe/H] abundance of our best model with $w = 0.5$ (in red) and data (in green). (c) The time evolution of the SFR predicted by our models for Enceladus with different values of w. Each vertical line labels the median stellar birth time of the corresponding model, and the shaded area indicates the $\pm 1\,\sigma$ region. (d) The time evolution of the stellar mass predicted by our models with different w for Enceladus.

predictions for the evolution of the SFR as a function of time, for our fiducial model, for different mass loading factors. By assuming for the age of the Universe $t_{\rm U}$ = 13.8 Gyr, and considering only the SFH from t = 0 to 4 Gyr, when the merger with the Galaxy approximately took place (Helmi et al. 2018), the median age of Enceladus stars from our model with $w = 0.5$ corresponds to $t_{\rm med} = 12.33^{+0.92}_{-1.36}$ Gyr. Assuming different mass loading factors does not significantly change our predictions for the median ages of the stars in Enceladus (see the different vertical lines in Fig. 2c); in particular, increasing the mass loading factor determines a slight increase also in the median stellar ages of the model.

Our predicted SFH in Fig. 2(c) globally accounts for the ages derived by Helmi et al. (2018), which are in the range 10-13 Gyr, and

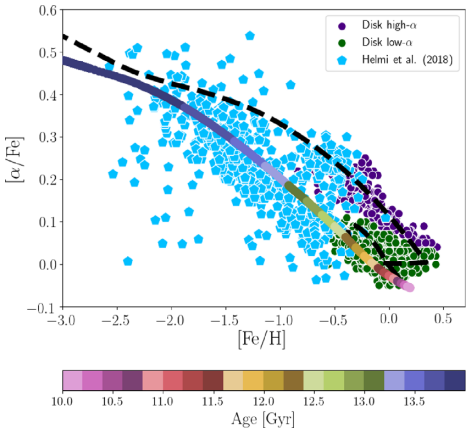

Figure 3. Observed [α/Fe]–[Fe/H] abundance diagram from Helmi et al. (2018) for Enceladus stars (light blue filled pentagons) along with the MW disc data from the APOKASC sample (high-α and low α sequence in purple and green points, respectively Silva Aguirre et al. 2018). The dashed black line represents the two-infall chemical evolution model of Spitoni et al. (2019), whereas the solid colour-coded line is our fiducial model for Enceladus, with the colour code indicating the predicted ages of the stars.

our best chemical evolution model is remarkably in agreement with Gallart et al. (2019), which find a median age of Enceladus stars $t_{\rm med}$ = 12.37 Gyr from isochrone-fitting, using a very different approach. Moreover, our results are also in agreement with the short SFR time-scales inferred by Fernández-Alvar et al. (2018) for their APOGEE sample of stars. Finally, in Fig. 2(d), we show the predicted evolution of the total stellar mass of Enceladus. In particular, the stellar and gas masses of Enceladus at $t_{\rm med}$ as predicted by our model with w = 0.5 are $M_{\star,\rm Enc} = 3.24 \times 10^9$ M$_\odot$ and $M_{\rm gas,Enc} = 6.62 \times 10^9$ M$_\odot$, respectively, with gas fraction ≈0.67. At the time of the merger with the Milky Way, therefore, we predict a stellar mass $M_\star \approx 5 \times 10^9$ M$_\odot$, in agreement with Belokurov et al. (2018) and Helmi et al. (2018).

In Fig. 3, we compare the observed data of Helmi et al. (2018) for [α/Fe]–[Fe/H] in Enceladus with the observed MW abundances of thick and thin-disc stars from the APOKASC sample (Silva Aguirre et al. 2018). In the figure, we also compare the predicted [α/Fe]–[Fe/H] chemical evolution track of the two-infall model of Spitoni et al. (2019) with our best model for Enceladus assuming w = 0.5, where the colour coding represents the predicted age of the stars in Enceladus. The model of Spitoni et al. (2019) is remarkable in the context of the two-infall chemical evolution models for the MW, because it has been developed to reproduce at the same time the observed age distribution of MW thick- and thin-disc stars from asteroseismic analysis of Kepler light curves (providing the most precise method to determine the stellar ages) and the chemical abundances from APOGEE, for a sample of stars in common between APOGEE and Kepler (Silva Aguirre et al. 2018).

In order to reproduce the observed bimodal distribution of MW thick- and thin-disc stars in [α/Fe]–[Fe/H], together with the distribution of the stellar ages, the model of Spitoni et al. (2019) revised the classical two-infall model for the MW of Chiappini, Matteucci & Gratton (1997), by assuming a second infall which started ≈9.4 Gyr ago, with a time delay of ∼4.5 Gyr after the beginning of the first infall. Such a time delay between the two infall episodes is much longer than that assumed by all previous two-infall chemical evolution models for the MW (Chiappini et al. 1997; Grisoni et al. 2017; Sahijpal & Kaur 2018), but it agrees with other recent independent studies, like Noguchi (2018) or Grand et al. (2018), which obtained very similar findings, but without attempting to fit also the observed age distribution of MW disc stars, as done in Spitoni et al. (2019). In summary, recent studies of the MW chemical evolution seem to agree that an extended hiatus in the Galactic SFH at high redshifts is required to reproduce the observed bimodality in the [α/Fe]–[Fe/H] between MW thick- and thin-disc stars.

By comparing the predicted age distribution of the stars in our best chemical evolution model for Enceladus and the predictions of the two-infall chemical evolution model of Spitoni et al. (2019) for the MW, we propose that the mechanism – which quenched the MW star formation at high redshifts, heating up the gas in the DM halo – was a major merger event with a satellite like Enceladus (see, for example, Gabor et al. 2010; Pontzen et al. 2017; Hunt et al. 2018; van de Voort et al. 2018 for the quenching mechanisms in galaxies, and Di Matteo et al. 2008; Martin et al. 2017; Wilson et al. 2019 for the effects of mergers on high-redshift galaxies).

We note that there might be a time-sequence problem between the age of the merger indicated by Helmi et al. (2018) (≈10 Gyr ago) and the findings of the two-infall model for the MW of Spitoni et al. (2019), where the second infall happened ≈9.4 Gyr ago (see their Fig. 2). However, a ∼10 per cent error in the ages of old stellar populations is well within the uncertainties of the most precise methods currently available for determining ages of field stars (e.g. asteroseismology; see also Silva Aguirre et al. 2018), and this can thereby conciliate the merger time from Helmi et al. (2018) with the Spitoni et al. (2019) model for the MW.

4 DISCUSSION AND CONCLUSIONS

We have presented the first attempt of modelling the chemical evolution of Enceladus, in order to reproduce the [α/Fe]–[Fe/H] abundance trend and the MDF observed by Helmi et al. (2018). Our fiducial model assumes SFE = 0.42 Gyr^{-1}, mass loading factors w = 0.5, infall time-scale $\tau_{\rm infall}$ = 0.24 Gyr, and infall mass $M_{\rm infall}$ = 10^{10} M$_\odot$. Our main findings and conclusions can be summarized as follows.

(i) We find for Enceladus a median iron abundance [Fe/H] = $-1.26^{+0.82}_{-1.06}$, obtained from the predicted galaxy SFH. Our result is in agreement with observations, which suggest a median iron abundance [Fe/H]$_{\rm obs} = -1.21^{+0.59}_{-0.49}$ (Helmi et al. 2018).

(ii) According to our results, the median age of Enceladus stars is $12.33^{+0.92}_{-1.36}$ Gyr, remarkably in agreement with Gallart et al. (2019), which estimated a median age ≈12.37 Gyr from isochrone-fitting analysis, by using a very different approach with respect to ours. We note that the position in the CMD of the stars with [Fe/H] = −1.3 (and [α/Fe] = 0.22) in the sample of Helmi et al. (2018) could be reproduced with isochrones of ∼13 Gyr.

(iii) The predicted age distribution of the stars from our best Enceladus chemical evolution model corroborates the time of the merger, occurring about 10 Gyr ago, estimated by Helmi et al. (2018), because the large majority of the stars in our best model have ages larger than 10 Gyr.

(iv) We predict that the stellar mass of Enceladus at the epoch of the merger suggested by Helmi et al. (2018) is $M_\star \approx 5 \times 10^9$ M$_\odot$, in agreement with the findings of Belokurov et al. (2018), Helmi et al. (2018), and Mackereth et al. (2019a), with a gas fraction ≈0.67 at the median age of Enceladus stars. The predicted Enceladus stellar mass is comparable with the predicted MW stellar mass from Spitoni et al. (2019) at the same epoch, which is $M_{\star,\rm MW} \approx 8 \times 10^9$ M$_\odot$.

Since we assume in our chemical evolution model for Enceladus an infall mass $M_{\rm infall} = 10^{10}\,{\rm M}_{\odot}$, it is unlikely that Enceladus alone provided sufficient gas mass to assemble the thin disc of our Galaxy.

(v) The merger between Enceladus and our Galaxy was likely the cause of a temporary quenching of the star formation and gas accretion in our Galaxy at high redshifts, which can be seen also in the predicted SFH of the two-infall model of Spitoni et al. (2019, see their fig. 4, upper panel) but also in the predicted bimodal SFH of the best MW-like galaxy in the cosmological hydrodynamical simulation of Grand et al. (2018), which is characterized by an extended quenching phase, occurring approximately at the same epochs of the merger indicated by Helmi et al. (2018), before the formation of the Milky Way thin disc. This temporal sequence is corroborated by our best model for Enceladus.

(vi) In the context of the two-infall chemical evolution model for the MW, it is likely that Enceladus was cannibalized by the Galaxy towards the end of the first infall episode, as a part of the gas and sub-structures of the infall episode itself. Nevertheless, before the collision between the MW and Enceladus happened, there might have been strong tidal interactions between the two galaxies as well, and this likely influenced the early accretion of gas from the IGM on to the Galaxy disc.

(vii) Further investigations are needed to confirm with different techniques and with higher precision the age distribution of the stars in Enceladus. Asteroseismology techniques currently provide the best way to probe stellar interiors, to determine with very high accuracy stellar ages (Casagrande et al. 2016; Silva Aguirre & Serenelli 2016; Miglio et al. 2017). In the future, asteroseismology combined with chemodynamical simulations will allow us to study the mass assembly history of our Galaxy with unprecedented temporal resolution, and this will be the subject of our future work.

Finally we note that an optimal chemical element to test different theories of halo formation may be barium (Spitoni et al. 2016), which is (relatively) easily measured in low-metallicity stars (see, for more details, Cescutti et al. 2006 and subsequent papers of the same author). In particular, Spitoni et al. (2016) demonstrated that the predicted [Ba/Fe]–[Fe/H] relation in dSphs and UfDs is quite different than that in the Galactic halo; it will be interesting, in the future, to investigate the abundance trends of neutron-capture s-process elements in Enceladus stars, to be compared with similar abundance trends in the MW galaxy.

ACKNOWLEDGEMENTS

We thank an anonymous referee for their comments, which greatly improved the clarity of this work. We thank T. Mackereth, J. Montalban, G. Iorio, and P. E. Nissen for interesting and stimulating discussions. FV and AM acknowledge support from the European Research Council Consolidator Grant funding scheme (project ASTEROCHRONOMETRY, G.A. n. 772293). ES and VSA acknowledge support from the Independent Research Fund Denmark (Research grant 7027-00096B). Funding for the Stellar Astrophysics Centre is provided by The Danish National Research Foundation (Grant agreement no.: DNRF106). FC acknowledges funding from the INAF PRIN-SKA 2017 program 1.05.01.88.04. FM acknowledges research funds from the University of Trieste (FRA2016).

REFERENCES

Belokurov V. et al., 2006, ApJ, 642, L137
Belokurov V., Erkal D., Evans N. W., Koposov S. E., Deason A. J., 2018, MNRAS, 478, 611
Bradamante F., Matteucci F., D'Ercole A., 1998, A&A, 337, 338
Bullock J. S., Kravtsov A. V., Weinberg D. H., 2001, ApJ, 548, 33
Casagrande L. et al., 2016, MNRAS, 455, 987
Cescutti G., François P., Matteucci F., Cayrel R., Spite M., 2006, A&A, 448, 557
Chiappini C., Matteucci F., Gratton R., 1997, ApJ, 477, 765
de Boer T. J. L., Belokurov V., Koposov S., 2015, MNRAS, 451, 3489
de Boer T. J. L., Belokurov V., Koposov S. E., 2018a, MNRAS, 473, 647
de Boer T. J. L., Belokurov V., Koposov S. E., Ferrarese L., Erkal D., Côté P., Navarro J. F., 2018b, MNRAS, 477, 1893
Deason A. J., Belokurov V., Koposov S. E., Gómez F. A., Grand R. J., Marinacci F., Pakmor R., 2017, MNRAS, 470, 1259
Di Matteo P., Bournaud F., Martig M., Combes F., Melchior A.-L., Semelin B., 2008, A&A, 492, 31
Di Matteo P., Haywood M., Lehnert M. D. et al., 2018, preprint (arXiv:1812.08232)
Fattahi A. et al., 2019, MNRAS, 484, 4471
Fernández-Alvar E. et al., 2018, ApJ, 852, 50
François P., Matteucci F., Cayrel R., Spite M., Spite F., Chiappini C., 2004, A&A, 421, 613
Gabor J. M., Davé R., Finlator K., Oppenheimer B. D., 2010, MNRAS, 407, 749
Gallart C., Bernard E. J., Brook C. B. et al., 2019, preprint (arXiv:1901.02900)
Grand R. J. J. et al., 2018, MNRAS, 474, 3629
Grisoni V., Spitoni E., Matteucci F., Recio-Blanco A., de Laverny P., Hayden M., Mikolaitis Ŝ., Worley C. C., 2017, MNRAS, 472, 3637
Hayes C. R. et al., 2018, ApJ, 852, 49
Haywood M., Di Matteo P., Lehnert M. D., Snaith O., Khoperskov S., Gómez A., 2018, ApJ, 863, 113
Helmi A., White S. D. M., 1999, MNRAS, 307, 495
Helmi A., White S. D. M., de Zeeuw P. T., Zhao H., 1999, Nature, 402, 53
Helmi A., Babusiaux C., Koppelman H. H., Massari D., Veljanoski J., Brown A. G. A., 2018, Nature, 563, 85
Hunt Q. et al., 2018, ApJ, 860, L18
Ibata R., Irwin M., Lewis G. F., Stolte A., 2001, ApJ, 547, L133
Iorio G., Belokurov V., 2019, MNRAS, 482, 3868
Klypin A., Kravtsov A. V., Valenzuela O., Prada F., 1999, ApJ, 522, 82
Koposov S. E., Belokurov V., Torrealba G., 2017, MNRAS, 470, 2702
Koposov S. E., Belokurov V., Li T. S. et al., 2019, MNRAS, 485, 4726
Kroupa P., Tout C. A., Gilmore G., 1993, MNRAS, 262, 545
Kruijssen J. M. D., Pfeffer J. L., Reina-Campos M., Crain R. A., Bastian N., 2019, MNRAS, 486, 3180
Mackereth J. T. et al., 2019a, MNRAS, 482, 3426
Mackereth J. T., Bovy J., Leung H. W. et al., 2019b, preprint (arXiv:1901.04502)
Majewski S. R., Skrutskie M. F., Weinberg M. D., Ostheimer J. C., 2003, ApJ, 599, 1082
Martin G., Kaviraj S., Devriendt J. E. G., Dubois Y., Laigle C., Pichon C., 2017, MNRAS, 472, L50
Matteucci F., Recchi S., 2001, ApJ, 558, 351
Miglio A. et al., 2017, Astron. Nachr., 338, 644
Morrison H. L., Mateo M., Olszewski E. W., Harding P., Dohm-Palmer R. C., Freeman K. C., Norris J. E., Morita M., 2000, AJ, 119, 2254
Myeong G. C., Evans N. W., Belokurov V., Amorisco N. C., Koposov S. E., 2018a, MNRAS, 475, 1537
Myeong G. C., Evans N. W., Belokurov V., Sanders J. L., Koposov S. E., 2018b, ApJ, 863, L28
Newberg H. J. et al., 2003, ApJ, 596, L191
Nissen P. E., Schuster W. J., 2010, A&A, 511, L10
Noguchi M., 2018, Nature, 559, 585
Padovani P., Matteucci F., 1993, ApJ, 416, 26
Placco V. M. et al., 2018, AJ, 155, 256
Pontzen A., Tremmel M., Roth N., Peiris H. V., Saintonge A., Volonteri M., Quinn T., Governato F., 2017, MNRAS, 465, 547
Prantzos N., 2008, A&A, 489, 525

Sahijpal S., Kaur T., 2018, MNRAS, 481, 5350
Sanders J. L., Das P., 2018, MNRAS, 481, 4093
Shipp N. et al., 2018, ApJ, 862, 114
Silva Aguirre V., Serenelli A. M., 2016, Astron. Nachr., 337, 823
Silva Aguirre V. et al., 2018, MNRAS, 475, 5487
Simion I. T., Belokurov V., Koposov S. E., 2019, MNRAS, 482, 921
Simon J. D., 2019, preprint (arXiv:1901.05465)
Spitoni E., Vincenzo F., Matteucci F., Romano D., 2016, MNRAS, 458, 2541
Spitoni E., Silva Aguirre V., Matteucci F., Calura F., Grisoni V., 2019, A&A, 623, A60
Ting Y.-S., Rix H.-W., 2019, preprint (arXiv:1808.03278)
van de Voort F. et al., 2018, MNRAS, 476, 122
Wilson T. J. et al., 2019, ApJ, 874, 18

This paper has been typeset from a TEX/LATEX file prepared by the author.